



1 **Impact of meteorological conditions on BVOC emission rate from Eastern**
2 **Mediterranean vegetation under drought**

3

4 Qian Li¹, Gil Lerner¹, Einat Bar², Efraim Lewinsohn², Eran Tas^{1*}

5 ¹ Institute of Environmental Sciences, The Robert H. Smith Faculty of Agriculture, Food and
6 Environment, The Hebrew University of Jerusalem, P.O. Box 12, Rehovot 7610001, Israel

7 ² Department of Vegetable Research, Agricultural Research Organization – Newe Ya'ar Center,
8 Israel

9

10

11 * Correspondence to:

12 Eran Tas, Institute of Environmental Sciences, The Robert H. Smith Faculty of Agriculture, Food
13 and Environment, The Hebrew University of Jerusalem, P.O. Box 12, Rehovot 7610001, Israel
14 eran.tas@mail.huji.ac.il



15 **Abstract**

16 A comprehensive characterization of drought's impact on biogenic volatile organic
17 compounds (BVOC) emissions is essential for understanding atmospheric chemistry under
18 global climate change, with implications for both air quality and climate model simulation.
19 Currently, the effects of drought on BVOC emissions are not well characterized. Our study
20 aims to test: i) whether instantaneous changes in meteorological conditions can serve as a
21 better proxy for drought-related changes in BVOC emission compared to the absolute
22 values of the meteorological parameters, as indicated in a companion article based on
23 BVOC mixing-ratio measurements; ii) the impact of a plant under drought stress receiving
24 a small amount of precipitation on BVOC emission rate, and on the manner in which the
25 emission rate is influenced by meteorological parameters. To address these objectives, we
26 conducted our study during the warm and dry summer conditions of the Eastern
27 Mediterranean region, focusing on the impact of drought on BVOC emissions from natural
28 vegetation. Specifically, we conducted branch-enclosure sampling measurements in Ramat
29 Hanadiv Nature Park, both under natural drought and after irrigation (equivalent to 5.5–7
30 mm precipitation), for six selected branches of *Phillyrea latifolia*, the highest BVOC
31 emitter in this park, in September–October 2020. The samplings were followed by gas
32 chromatography-mass spectrometry analysis for BVOCs identification and flux
33 quantification. The results corroborate the finding that instantaneous changes in
34 meteorological parameters, particularly relative humidity (RH), offer the most accurate
35 proxy for BVOC emission rates under drought, compared to the absolute values of either
36 temperature (T) or RH. However, after irrigation, the correlation of the detected BVOC
37 emission rate with the instantaneous changes in RH became significantly more moderate,



38 or even reversed. Our findings highlight that under drought, the instantaneous changes in
39 RH, and to a lesser extent in T, are the best proxy for the emission rate of monoterpenes
40 (MTs) and sesquiterpenes (SQTs), whereas under moderate drought conditions, T or RH
41 serves as the best proxy for MT and SQT emission rate, respectively. In addition, the
42 detected emission rates of MTs and SQTs increased by 150% and 545%, respectively, after
43 a small amount of irrigation.

44

45 **1 Introduction**

46 Biogenic volatile organic compounds (BVOCs) are released by plants and other organisms
47 to the atmosphere. They play a critical role in both climate change and photochemical air
48 pollution (Cai et al., 2021; Calfapietra et al., 2013; Curci et al., 2009; Guenther, 2013;
49 Kesselmeier and Staudt, 1999; Peñuelas et al., 2009). BVOCs are thought to be emitted by
50 plants as a defense mechanism against biotic and abiotic stresses, such as herbivory and
51 high temperatures (Berg et al., 2013; Blande et al., 2007; Brilli et al., 2009; Peñuelas and
52 Munné-Bosch, 2005). BVOCs may also be involved in plant–plant and plant–animal
53 communication, allowing plants to signal to other organisms about their response to
54 environmental conditions (Baldwin et al., 2006; Filella et al., 2013; Niinemets and Monson,
55 2013).

56 The emission rate and composition of BVOCs can vary widely depending on
57 various factors, such as meteorological conditions, rate of synthesis, and physicochemical
58 properties (Niinemets and Monson, 2013). Climate change is expected to significantly
59 impact BVOC emission rate and composition. As temperature rises, the emission rate of
60 most BVOCs increases in an Arrhenius-type manner (Goldstein et al., 2004; Greenberg et



61 al., 2012; Guenther et al., 1995; Monson et al., 1992; Niinemets et al., 2004; Tingey et al.,
62 1990). On the other hand, drought can have a more complex effect on the emission and
63 composition of BVOCs. Depending on the type of vegetation, the level of drought stress,
64 and additional ambient conditions, the emission of BVOCs can be partially or completely
65 suppressed (Fortunati et al., 2008; Holopainen and Gershenson, 2010; Llusia et al., 2016;
66 Peñuelas and Staudt, 2010; Schade et al., 1999), or enhanced in a way that has not yet been
67 characterized (Fitzky et al., 2023; Geron et al., 2016; Potosnak et al., 2014).

68 The effect of drought on isoprene emission has been extensively studied, and it was
69 discovered to be postponed relative to, and/or less significant than the effect on
70 photosynthetic rate (Asensio et al., 2007; Brilli et al., 2007; Fortunati et al., 2008;
71 PEGORARO et al., 2006; Ryan et al., 2014). However, whereas under moderate drought
72 stress, isoprene emission may only slightly decrease or increase, it was shown to decrease
73 considerably under severe or prolonged drought stress (Fortunati et al., 2008; Han et al.,
74 2022; Jiang et al., 2018). The impact of drought on the emission of other BVOCs, such as
75 monoterpenes (MTs) and sesquiterpenes (SQTs), has been less studied.

76 The Eastern Mediterranean has a unique climate characterized by a hot and dry
77 summer, making it an ideal location to study the impact of drought on BVOC emissions.
78 The semiarid and arid regions are particularly vulnerable to climate change, and climate
79 simulations predict that the Eastern Mediterranean region will experience more frequent
80 and severe droughts in the future (Giorgi and Lionello, 2008; Lionello, 2012). Research
81 conducted in Israel has investigated the impact of drought on BVOC emissions from a
82 range of local plant species. For example, Llusia et al. (2016) examined the effect of
83 drought on terpene emission from Yatir Forest, a pine forest in the northern Negev. They



84 found that some of the MT and SQT emissions increased under moderate drought
85 conditions but strongly decreased under severe drought conditions. Another measurement
86 by Li et al. (2023), performed in late autumn 2016 in Shibli Forest in northern Israel, found
87 that under severe drought stress, BVOC emissions respond more significantly to the
88 instantaneous changes in meteorological parameters (especially relative humidity [RH])
89 than to the meteorological parameters themselves. These studies suggest that the impact of
90 drought on BVOC emissions is not well-characterized and varies in a complex manner,
91 depending on plant species, BVOC type, and meteorological parameters, such as
92 temperature (T) and RH, as well as the level of drought stress. Hence, more research is
93 needed to better characterize the effect of drought on BVOC emission rates and
94 composition, which can in turn improve air quality and climate modeling.

95 In this study, we use the severe drought conditions during the autumn in the Eastern
96 Mediterranean to study the effect of drought on the emission of BVOCs from natural
97 vegetation. The main specific objectives of this study were to: i) identify whether
98 instantaneous changes in meteorological parameters can serve as a better proxy for BVOC
99 emission rates under drought than their absolute values, and ii) determine the extent to
100 which small precipitation amounts, under drought conditions, can impact BVOC emission
101 rates and the manner in which the emission rate is influenced by meteorological parameters.

102

103 **2 Methods**

104 We used an enclosure-based measurement system to quantify BVOC emissions, allowing
105 for direct measurement of BVOC fluxes at the branch level. The measurements were
106 performed in autumn under the prolonged drought stress conditions typical to this region.



107 BVOC measurements in the Eastern Mediterranean are rare, and to the best of our
108 knowledge, our study is the first to apply direct measurements of BVOC flux from specific
109 branches of natural vegetation in this region. Plants were sampled before and after the
110 application of a small amount of irrigation to study the response of BVOC emissions, under
111 exposure to natural drought conditions, to a small amount of precipitation. This was
112 followed by gas chromatography–mass spectrometry (GC–MS) to identify and quantify
113 the emitted BVOCs. Closed chambers are often used for measurements of BVOCs at the
114 branch level (Duhl et al., 2008). Compared to open-system methods, the enclosure-based
115 system (including a glass cuvette or Tedlar bag) can focus on specific vegetation in a more
116 controlled manner. To investigate the effects of drought on BVOC emission rates and
117 composition, we performed two sets of measurements – before and after irrigation – for
118 comparison. To study the effect of meteorological conditions on BVOC flux, we monitored
119 meteorological parameters inside the bag and at a meteorological station that was 300–600
120 m from the branches.

121

122 *2.1 Sampling site and studied species*

123 The on-site branch measurements were conducted at Ramat Hanadiv Nature Park (32°
124 33' 19.87" N, 34° 56' 50.23" E), 3.6 km from the Eastern Mediterranean seashore and
125 exposed to a typical Eastern Mediterranean climate, with annual precipitation of 640 mm
126 (averaged over the last 5 years, and occurring mainly between November and March). The
127 vegetation at the site is dominated by mixed Mediterranean shrubbery. More details about
128 the site and vegetation can be found in Li et al. (2018) and Dayan et al. (2020). The
129 measurements were conducted at the end of summer/beginning of autumn under drought



130 conditions. No precipitation was recorded for 108 days between 24 May 2020 and the
131 beginning of the study on 9 Sep 2020.

132 *Phillyrea latifolia* (broad-leaved phillyrea), identified as the greatest BVOC-
133 contributing plant species in the Ramat Hanadiv natural park, was sampled. The species is
134 native to the Mediterranean Basin and belongs to the family Oleaceae. In Ramat Hanadiv,
135 it accounts for 7.5% of all vegetation, but up to ~35% of all BVOC emissions, according
136 to the Model of Emissions of Gases and Aerosols from Nature (MEGAN v2.1; Dayan et
137 al., 2020; Guenther et al., 2012; Li et al., 2018). The selected plants were mature and did
138 not show any visible signs of senescence. Sampled branches were shaded, to eliminate the
139 effect of non-natural high temperature in the enclosure system, and measurements were
140 performed at 1.5 to 2 m aboveground.

141

142 ***2.2 Branch-enclosure sampling system and setup***

143 Figure 1 presents a self-made branch-sampling system was used for this study. All tubes
144 and connections are Teflon, while valves and flowmeters are stainless steel. A compressor
145 provides a controllable rate of ambient air flow through an adjustable T-junction valve (to
146 adjust the flow rate) to a zero-air device (Model 1150 dual reactor, Thermo Fisher
147 Scientific, Waltham, MA, USA), which includes a catalytic converter heated to ~350 °C to
148 oxidize CO and HC to CO₂ and H₂O. From the zero-air device, the air flows through a
149 copper coil to cool it down, and then through a mass flowmeter into a Tedlar bag (CEL
150 Scientific Corporation, Cerritos, CA, USA), at a flow rate of about 7 L min⁻¹ (monitored
151 by flowmeter A), a high enough inflow to produce slight overpressure inside the bag. The
152 inert and light-transparent 10 L Tedlar bag is tied tightly around a tree branch, along with



169 (7890A/5975C) system (Santa Clara, CA, USA) equipped with a Stabilwax column
170 (Restek, 30 m, 0.25 mm ID capillary column; polyethylene glycol, 0.25 μm film thickness).
171 The general run parameters were as follows: injector, 230 $^{\circ}\text{C}$; column oven, initial
172 temperature of 45 $^{\circ}\text{C}$ for 5 min, followed by a ramp of 5 $^{\circ}\text{C min}^{-1}$ to 120 $^{\circ}\text{C}$, 20 $^{\circ}\text{C min}^{-1}$
173 to 240 $^{\circ}\text{C}$ final, and 5-min hold with a total run time of 31.5 min; carrier gas, He 32 psi;
174 mass spectrometer ionization energy, 70 eV; m/z, 41 to 300; scan time, 5.4 s. The
175 chromatograms were analyzed using MassHunter Quant Analysis (B.10.00, Agilent
176 Technologies, Santa Clara, CA, USA) software. Compounds were identified by comparing
177 their relative retention indices and mass spectra with those of authentic standards or those
178 found in the literature, supplemented with W10N14 and 2205 GC–MS libraries.

179 We chose to analyze the most abundant BVOC species: *cis*- β -ocimene (E, Z) (MT),
180 and β -caryophyllene, α -humulene, α -farnesene, germacrene-D (SQTs). For calibration,
181 analytical-grade standard solutions (7–12 concentrations) were prepared, ranging in
182 concentrations from 0.25 to 1000 ng mL^{-1} by diluting known masses of pure chemicals
183 with methanol. The calibration analytes were injected using a GC syringe onto clean
184 sorbent tubes connected to a calibration solution-loading rig (Markes International) at a
185 nitrogen flow of 80 mL min^{-1} . The standards for the BVOC species were *cis*- β -ocimene (E,
186 Z) (W353977, Sigma-Aldrich) (MT), and β -caryophyllene (22075-1ML-F, Sigma-
187 Aldrich), α -humulene (PHL83351, Sigma-Aldrich), α -farnesene (Biosynth® Carbosynth
188 Ltd., UK), germacrene-D (Toronto Research Chemicals, Canada) (SQTs). All standard-
189 loaded tubes were prepared in triplicate and results were averaged. The loaded tubes were
190 analyzed under the same conditions used for the other samples. Standard curves of peak
191 area counts vs. VOC mass (μg) were fitted using linear regression analyses; both yielded



192 high regression coefficients ($r^2 \geq 0.99$ in most cases). More details on the calibration are
193 provided in Sect. S1.

194

195 ***2.4 Experimental setup***

196 ***2.4.1 Branch sampling, meteorological parameter measurements and flux evaluation***

197 The field measurements were performed from late summer to early autumn – 9 Sep to 27
198 Oct 2020. Samplings were conducted on six selected *Phillyrea latifolia* branches on
199 different bushes. Each branch was measured over two sequential days: 8–9 Sep, 14–15 Sep,
200 22–23 Sep, 12–13 Oct, 19–20 Oct, and 26–27 Oct. The bushes were at least 20 m apart, to
201 enable selective irrigation for individual shrubs. Meteorological parameters were measured
202 at a distance of 300–600 m from the branch measurements. These parameters included T
203 and RH, measured using a Campbell HC2S3 probe; net radiation, measured with a CNR4
204 Kipp & Zonen net radiometer; and wind speed and direction, recorded by a 05103 R.M.
205 Young sensor. Eight 30-min samplings were performed per measurement day. In addition,
206 two reference samplings were performed with full equipment setup, but no branch inside
207 the bag. These reference samplings were performed before and after the eight
208 measurements. Prior to the first reference sampling, the system and branches were given
209 at least 60 min to adapt to the different conditions after the setup of the bag and equipment.
210 Following the 10th sampling on the second measurement day of each 2-sequential-day
211 period, the sampled branch was cut and sent to the laboratory for leaf analysis. Leaf net dry
212 weight and area were evaluated within 24 h after cutting the branch. All leaves were
213 scanned, and a digital color-based image-processing method was used to identify the total
214 (RGB values: 40–200, 50–200, 30–200) and healthy (RGB values: 40–110, 50–105, 30–



215 80) leaf areas. The leaves were then dried for 72 h at 60 °C, and their dry weight was
216 recorded.

217 The sampling tubes were kept in a cooler with a temperature below 5 °C after the
218 measurement, and analyzed within 5 days of sampling by GC–MS (see Sect. 2.3). Of the
219 identified species, the MT and four SQT compounds with the highest sampled mass (*cis*-
220 β -ocimene, β -caryophyllene, α -humulene, α -farnesene, and germacrene D) were chosen
221 for quantification by GC–MS (see Sect. 2.3).

222 The emission rate of BVOCs per leaf area, E_A ($\text{ng cm}^{-2} \text{h}^{-1}$), for a branch was
223 evaluated by the following formula:

$$224 \quad E_A = \left(m \frac{F_{in-B}}{F_{out-T}} \right) / (A \cdot t) \quad (1)$$

225 where m (ng) is the evaluated mass of any BVOC compound inside the tube, F_{in-B} (L min^{-1})
226 ¹) and F_{out-T} (mL min^{-1}) are the flow rate pumped into the bag and the flow rate through
227 the adsorbent tube, respectively, A (cm^2) is the total leaf area of the branch, and t (h) is the
228 sampling time.

229 The emission rate of BVOCs per biomass, E_M ($\text{ng g}^{-2} \text{h}^{-1}$), was evaluated by:

$$230 \quad E_M = \left(m \frac{F_{in-B}}{F_{out-T}} \right) / (M \cdot t) \quad (2)$$

231 where M (g) is the leaf biomass of the branch.

232

233 **2.4.2 Irrigation and soil-water content quantification**

234 Manual irrigation was applied at the end of the first measurement day of each 2-sequential-
235 day measurement period (see Fig. 2). The irrigation amounts were 50–70 L within a radius
236 of 1–2 m from the stem of the plants used for sampling (equivalent to 5.5–7 mm rain). This

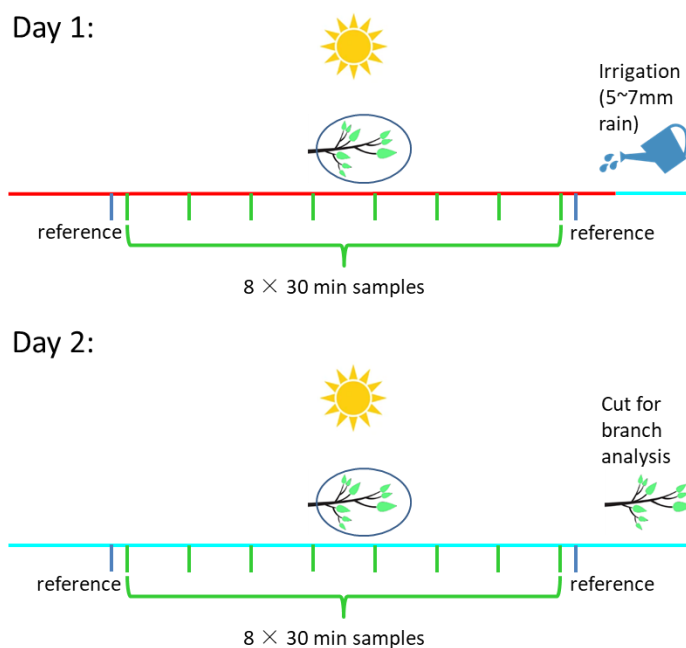


237 irrigation served to identify the potential effect of a small precipitation event during a
 238 drought period on BVOC emission rate and composition.

239 Ten soil samples were collected at solar noon time within 2 m from the sampled
 240 plant on every experimental day. To evaluate the soil-water content, soil samples were
 241 weighed on the day of collection, and weighed again after drying them in an oven at 105 °C
 242 for 24 h. The following formula was used to calculate the soil-water content:

243
$$w = \frac{M_{tot} - M_{dry}}{M_{dry}} \times 100\% \quad (3)$$

244 where w (g/g) is the soil gravimetric water content and M_{tot} (g) and M_{dry} (g) are the total
 245 and dried soil mass, respectively.



246 **Figure 2.** Schematic of the experimental design. Day 1 and Day 2 represent, respectively, the first and
 247 second day of each two-sequential-day sampling period for a specific branch. Green and blue bars represent
 248 sampling measurements and reference measurements, respectively. The red and cyan lines mark sampling
 249 prior to manual irrigation on Day 1 and after manual irrigation, on Day 2, respectively.

250



251 **2.4.3 Correlation between BVOC emission rate and temporal changes in RH and T**

252 To test the effect of instantaneous changes in RH and T on the emission rate of the sampled
253 BVOCs, we studied the correlation between the temporal changes in both ambient air RH
254 and T with the BVOC emission rate during the sampling. BVOC sampling length was 30
255 min, with a gap of 1 h between each sampling. To account for instantaneous changes in
256 RH and T we introduce δ_{RH} and δ_T , respectively. δ_{RH} is defined as follows:

257
$$\delta_{RH} = \sum_{i=1}^n \left(\frac{RH_{i+1}}{RH_i} - 1 \right) \quad (4)$$

258 where i is the 10 min time step, and n is the number of time steps.

259 δ_T is defined in the same manner as follows:

260
$$\delta_T = \sum_{i=1}^n \left(\frac{T_{i+1}}{T_i} - 1 \right) \quad (5)$$

261 The correlations between δ_{RH} , δ_T and the BVOC fluxes for all samples were tested
262 for different values of n . In a preliminary test, it was found that the highest average
263 correlations of δ_{RH} and δ_T with BVOC emission rate were obtained when $n = 9$.
264 Accordingly, the calculation duration of δ_{RH} and δ_T began 60 min before each 30 min
265 BVOC emission rate sampling. This finding is consistent with a similar analysis conducted
266 by Li et al. (2023). Similarly, the correlation between δ_{RH} and δ_T and BVOC emission rate
267 in that study applied δ_{RH} and δ_T which were calculated for 90 min cycles, while the
268 beginning of each cycle was 60 min prior to the beginning of each compatible 30 min
269 BVOC sampling.

270

271 **2.4.4 Afternoon emission trend (AET) analysis**

272 Under drought conditions, the increased stomatal resistance can largely reduce the BVOC
273 emission rate (see Sect. 1). Accordingly, it was found that the BVOC mixing ratio tends to



274 reach a minimum around noontime when RH tends to reach its daily minimum and stomatal
275 conductance is limited (Nobel, 1999), and then gradually increase in the afternoon (Li et
276 al., 2023). Our observations indicated a clear increase in BVOC emission rates during the
277 afternoon for the days before the irrigation. On those days, no clear decrease in BVOC
278 emission was observed before noon; instead, the BVOCs generally exhibited lower
279 emission rates. Here we introduce a method for quantifying the trend of emission rate right
280 after the mid-day minimum, which applies the afternoon emission trend (AET) index:

$$281 \quad \text{AET} = \sum_{i=1}^n \left(\frac{E_{i+1}}{E_i} - 1 \right) \quad (6)$$

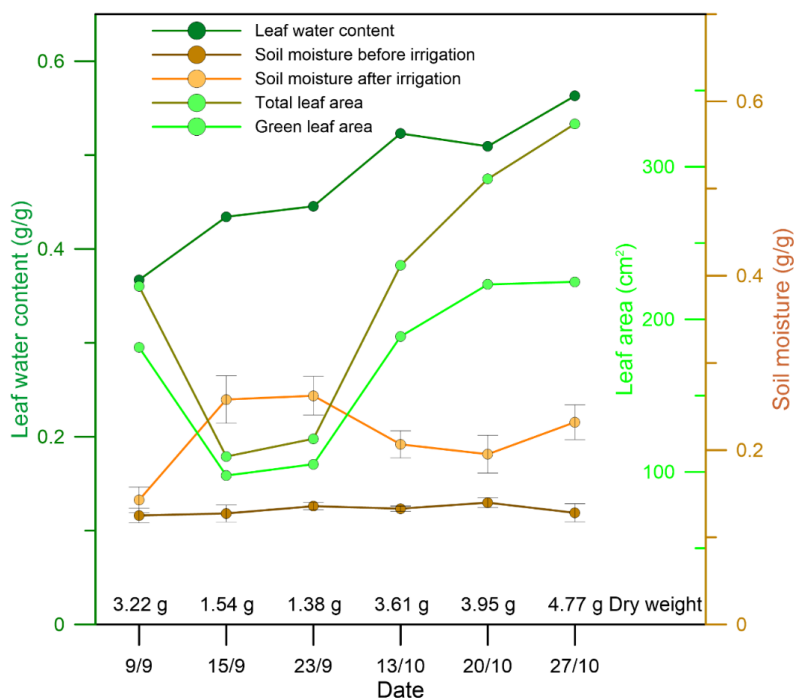
282 where E_i is the emission rate of the i_{th} sample, while $i = 1$ indicates the daily minimum
283 around noontime, between 12:00–14:00 h. Hence, the AET indicates the trend and
284 magnitude of the emission in the afternoon of any measurement day.

285

286 **3 Results and discussion**

287 ***3.1 Analysis of branch leaves***

288 Figure 3 shows the total leaf area (cm^2), green leaf area (cm^2), leaf water content, and soil
289 moisture before and after irrigation of each sampling branch. Leaf green area ranged
290 between 68% to 89% of the total leaf area. Soil moisture was around 12.5–14.0% before
291 irrigation and ~14.3–26.2% after irrigation. Interestingly, the leaf water content after
292 irrigation increased gradually during the experimental period, indicating that the capacity
293 for water uptake from the soil increases with drought prolongation.



294 **Figure 3.** Properties of the sampled branch leaves and soil moisture within a radius of 1 m from the stem of
 295 the sampling plant. Presented leaf property values are averages over all sampled branch leaves.

296

297 **3.2 Emission rates of MTs and SQTs**

298 Whereas previous branch enclosure studies focused primarily on isoprene emissions
 299 (Genard-Zielinski et al., 2015; Genard-Zielinski et al., 2018; Saunier et al., 2017), our
 300 measurements did not detect large amounts of isoprene emissions from the selected
 301 *Phillyrea latifolia*, in line with previous studies showing that some plant types do not emit
 302 notable amounts of isoprene (Aydin et al., 2014; Bracho-Nunez et al., 2013). Our analysis
 303 focused on the MTs and SQTs detected in our observations, as described in the following
 304 section.

305



306 **3.2.1 MTs**

307 On all 10 sampling days for which MTs were identified, the 5 days prior to irrigation were
308 under drought conditions (i.e., more than 100 days after the last precipitation event), and 5
309 days were under irrigation conditions on the same branches (see Sect. 2.4.2). The branch
310 which was sampled on Sep 14–15 did not show any detectable MT emission. The diurnal
311 emission fluxes of MTs from the branches are shown in Fig. 4.

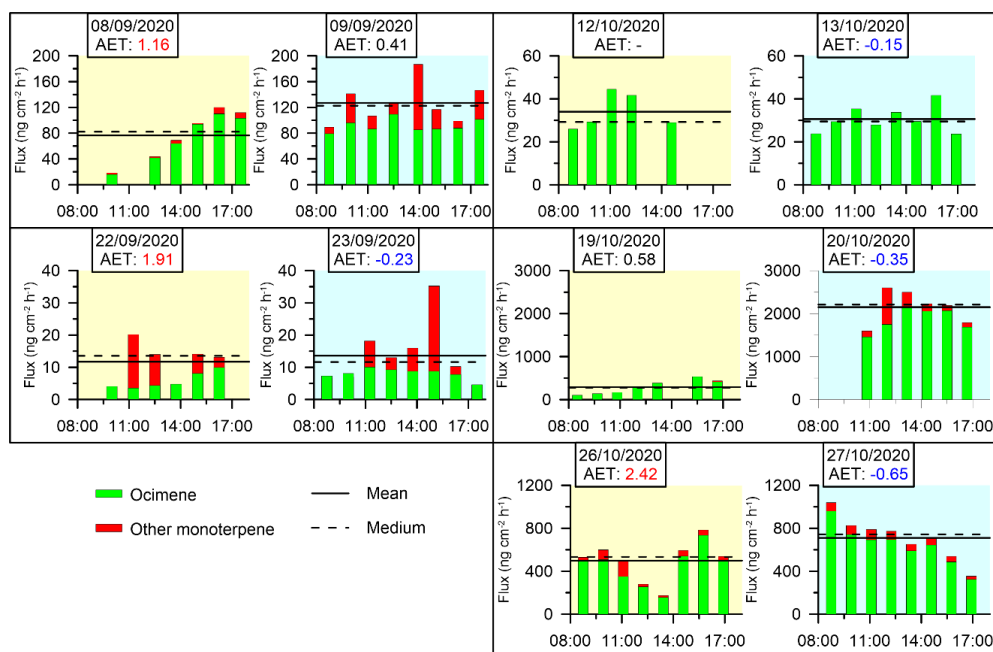
312 The daily average emission rate of MTs over all sampling days ranged from 11.7–
313 2151.4 ng cm⁻² h⁻¹ (0.89–121.5 μg g⁻¹ h⁻¹), with *cis*-β-ocimene being most abundant at 88%
314 of all detected MTs. These MT emission rates are similar to previous branch enclosure
315 studies, which were conducted predominantly between May and October under Western
316 Mediterranean conditions, where they ranged from 0 to approximately 140 μg g⁻¹ h⁻¹
317 (Bracho-Nunez et al., 2013; Llusà and Peñuelas, 2000; Núñez et al., 2002; Owen et al.,
318 1997; Owen and Hewitt, 2000; Staudt et al., 2001; Street et al., 1997). Less information is
319 available on the emission rates of MTs in the Eastern Mediterranean. Aydin et al. (2014)
320 used a branch enclosure system to detect emission rates ranging from 0.0047 to 14.2 μg g⁻¹
321 h⁻¹ in 14 different forested areas in Turkey. Seco et al. (2017) quantified MT emissions
322 using eddy covariance method in pine forests in Israel, studying a semiarid site (Yatir) and
323 a Mediterranean sub-humid site (Birya) in the spring. Emission fluxes were found to
324 average at 40 ng cm⁻² h⁻¹ (Yatir) and 100 ng cm⁻² h⁻¹ (Birya), with peak values of 100 (Yatir)
325 and 190 (Birya) ng cm⁻² h⁻¹, while the daytime standardized MT emission capacities were
326 similar across both sites.

327 In our study, MT emissions under drought conditions ranged from 11.7 ng cm⁻² h⁻¹
328 to 499.0 ng cm⁻² h⁻¹, which is somewhat higher than other values reported in the Eastern



329 Mediterranean. It is important to note that differences in emission rates between our study
330 and the previously reported values in this region might be attributed to the different
331 measurement methodologies employed. Following irrigation, the mean daily MT emission
332 rates increased in four out of the five investigated branches, and ranged from 13.6 ng cm^{-2}
333 h^{-1} to $2151.4 \text{ ng cm}^{-2} \text{ h}^{-1}$. This reflects an average 150% increase for all sampling days in
334 the range of emission rates following irrigation, indicating that even a small amount of
335 water during a period of drought stress can significantly influence MT emissions. This
336 effect may be related to the dramatic increase in stomatal conductance, due to the increase
337 in water availability following irrigation (Medrano et al., 2002; Miyashita et al., 2005;
338 Vilagrosa et al., 2003).

339 AET (Sect. 2.4.4) values specified in figures 4 and 5 reinforced the significant
340 effect of small irrigation amounts on BVOC emission rates under drought, considering that
341 on drought days, AETs were high and positive, whereas after irrigation, AETs became
342 moderate or negative. This observation is consistent with previous studies showing that the
343 emission of BVOCs can be affected by the vegetation's stomatal activity, which tends to
344 be lower around noontime during drought stress (Li et al., 2023; Seco et al., 2017). Stomatal
345 resistance is typically two orders of magnitude larger than cuticular resistance (Nobel, 1999)
346 and therefore, the midday minimum and the following increase in MT emissions under
347 drought conditions may be mostly due to stomatal resistance, which can limit the exchange
348 of gases between the plant and the atmosphere. In other words, the increased emission of
349 MTs after irrigation may be due to reopening of the stomata, which allows for the release
350 of VOCs.



351 **Figure. 4** Branches' diurnal MT emission fluxes. No MTs were detected for the branch sampled on 14–15
 352 Sep. Yellow and blue shading indicate the days before and after irrigation, respectively (see Sect. 2.4.2).
 353 Horizontal solid and dashed lines are daytime mean and median fluxes of MTs, respectively. AET values
 354 (see Sect. 2.4.4) are marked in red and blue when they are larger than 1 or negative, respectively.

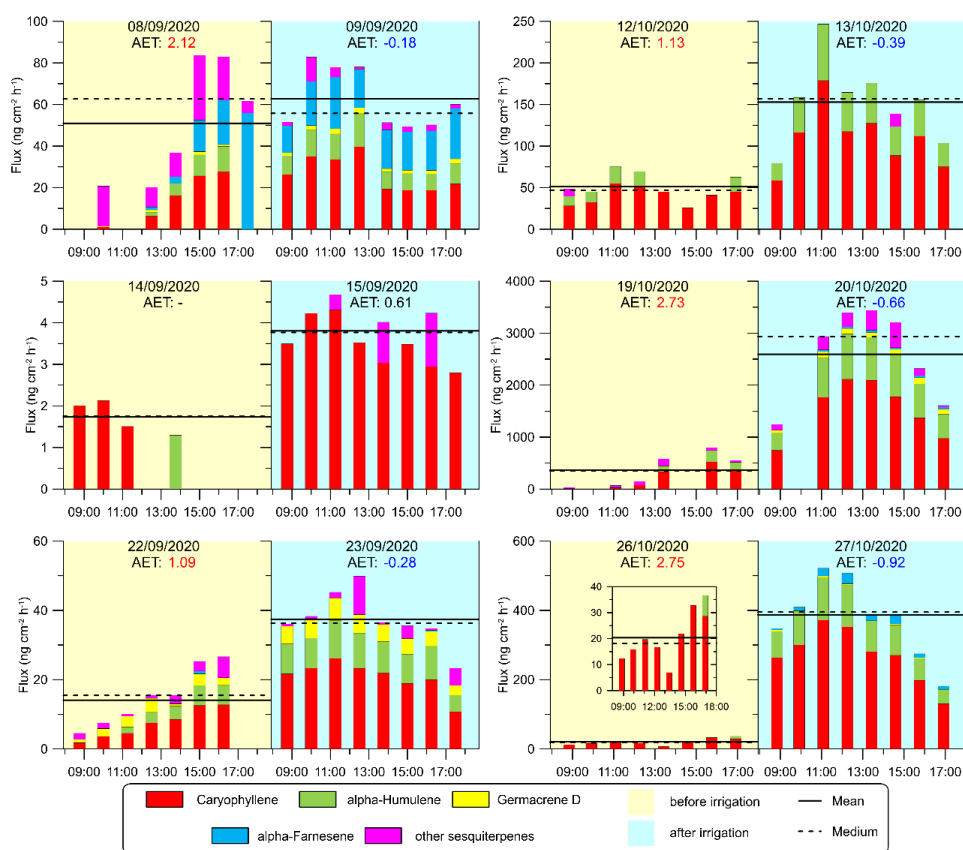
355

356 3.2.2 SQTs

357 Figure 5 shows the emission fluxes of SQTs for the branches under drought and irrigation
 358 conditions. The four major SQTs detected were β -caryophyllene, α -humulene, germacrene
 359 D, and α -farnesene. The daily average emission rate of SQTs ranged from 1.7–2595.7
 360 $\text{cm}^{-2} \text{h}^{-1}$ (0.11 – $146.6 \mu\text{g g}^{-1} \text{h}^{-1}$). In contrast to MTs, few studies provide branch enclosure
 361 measurements for SQTs. Notably, our study found significantly higher emission rates than
 362 previous research conducted between June and October under Eastern Mediterranean
 363 conditions, where rates ranged from 0.0011 to $0.63 \mu\text{g g}^{-1} \text{h}^{-1}$ (Aydin et al., 2014; Bracho-
 364 Nunez et al., 2013). The emission fluxes of the SQTs were overall comparable to those of



365 the MTs, which is a notable finding, considering that SQT emission rates are frequently
 366 around a quarter of the MT flux (Saunders et al., 2003; Sindelarova et al., 2014). The
 367 finding of relatively high SQT emission rates appears to be in line with the findings of Li
 368 et al. (2023), who reported relatively high mixing ratios of SQTs (33.6 times higher than
 369 isoprene, and 18.9 times higher than MTs) under drought conditions in the same region.



370 **Figure. 5** Diurnal SQT emission fluxes from the sampled branches. Column colors represent the emission
 371 fluxes of four types of SQTs, and the magenta section of the columns refers to other SQTs. Yellow and blue
 372 shading indicate the days before and after irrigation, respectively (see Sect. 2.4.2). Horizontal solid and
 373 dashed lines are daytime mean and median SQT flux rates, respectively. AET values (see Sect. 2.4.4) are
 374 marked in red and blue when they are larger than 1 or negative, respectively. To better present the trend on
 375 26 Oct, a smaller figure with a smaller scale is added.



376 Furthermore, we found that the increase in SQT emission flux following irrigation
377 (by 545% on average) was more significant than that of the MTs (by 150% on average).
378 This suggests that the response of SQT emissions to water availability is stronger than that
379 of MTs, which could be related to the chemical properties and physiological functions of
380 SQTs in plants. Bonn et al. (2019) found that a sharp increase in SQT emission occurs
381 close to the wilting point to protect the plant against oxidative damage, as also supported
382 by Caser et al. (2019). The latter found that drought can induce the SQT-synthesis
383 mechanism. The strong increase in SQT emission after irrigation in our study further
384 supports the notion that enhanced synthesis of SQTs occurs shortly after the release of
385 drought stress.

386 Interestingly, the high SQT emission rates found in this study are consistent with
387 the findings of a previous study conducted in the same area (Li et. al., 2023), which also
388 reported higher emission fluxes of SQTs compared to other studies. This suggests that there
389 may be a unique level of drought or plant characteristics that contribute to the high emission
390 fluxes of SQTs in this region.

391

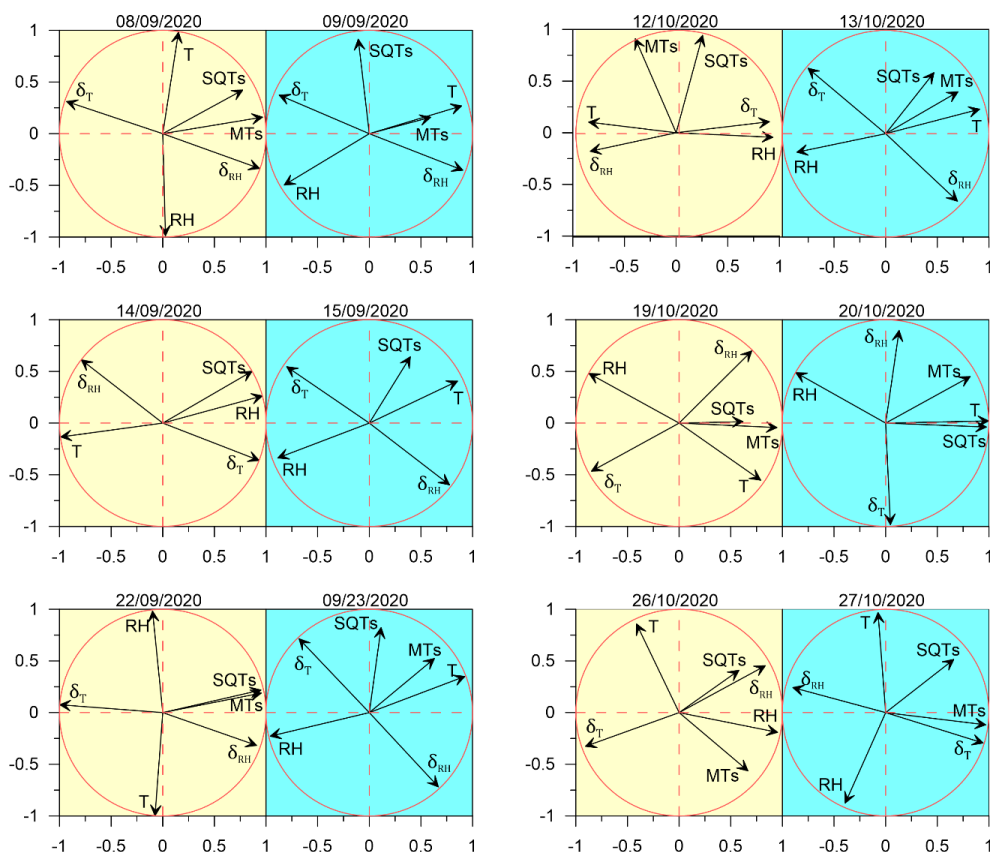
392 ***3.3 The impact of meteorological parameters on MT and SQT emission rates under*** 393 ***drought condition***

394 The effect of meteorological conditions on BVOC emission rate under drought conditions
395 is complex and depends on many factors, including vegetation type, BVOC type, and
396 ambient stress. In the Eastern Mediterranean region, Li et al. (2023) found that under
397 drought, the best proxy for BVOC emission is the instantaneous temporal change in RH;
398 temporal changes in T were also better correlated with BVOC mixing ratio than absolute



399 values of T. Here, we examined the impact of instantaneous changes in ambient air RH and
400 $T - \delta_{RH}$ and δ_T , respectively (see Sect. 2.4.3), as well as of ambient air T and RH on the
401 BVOC emission rate. Figure 6 presents a principal component analysis (PCA) for the
402 correlation of both δ_{RH} and δ_T with the BVOC emission rates. Before irrigation, when the
403 plants were under drought, on 8 Sep, 22 Sep, 19 Oct, and 26 Oct, the emission rates of both
404 MTs and SQTs were better correlated with δ_{RH} and δ_T (average Pearson's value (r) of
405 0.56 and -0.61, respectively) than with RH and T (r of -0.22 and 0.29, respectively).
406 Exceptional are 14 Sep and 12 Oct, also sampled under drought conditions: on 14 Sep, the
407 SQT emissions showed the best correlation with RH ($r = 0.97$); on 12 Oct, the emission
408 rates of BVOCs tended not to correlate with any of the tested meteorological parameters
409 because of a strong correlation of T and δ_{RH} ($r = -0.98$).

410 When focusing only on the days after irrigation, except for 27 Oct, the BVOC
411 emissions were better correlated with T (on average, $r = 0.52$) than with any other
412 parameter. Interestingly, on 27 Oct, the SQTs tended to correlate with RH (-0.58), while
413 the MT emission was better correlated with δ_T (0.94). The PCA results show some
414 similarities between the different sampled branches, in their stronger response to δ_{RH} than
415 to the other tested meteorological parameters and their almost complete lack of correlation
416 with T when under drought conditions. However, after irrigation, all BVOC emission rates
417 were highly responsive to T, more than to any other parameter, reflecting the well-known
418 Arrhenius-type increase for BVOC emission with temperature, as mentioned in Sect. 1
419



420 **Figure. 6** PCA analysis for the response of SQTs and MTs to meteorological parameters. The results are
 421 presented for SQTs, MTs, T, RH, δ_T , and δ_{RH} , individually for each measurement day. The yellow and
 422 blue shaded areas refer to the day before and after irrigation, respectively.

423

424 Table 1 summarizes the correlation coefficients between the emission rates of
 425 SQTs/MTs and RH, T, δ_{RH} , and δ_T , both before and after irrigation. Considering the
 426 significant variability in the emission rates of SQTs and MTs across different branches, the
 427 r values presented in the table are averages calculated from individual branch-level r values,
 428 separately before and after irrigation. Li et al. (2023) showed that under drought conditions,
 429 the temporal gradient of meteorological parameters in general was more strongly correlated



430 with BVOC emission rates – not only for RH, but also for T and vapor-pressure deficit.
 431 Before irrigation, both SQT and MT emission rates were more strongly correlated with δ_{RH}
 432 and δ_T than with RH and T. However, after irrigation, the r values for the correlations with
 433 δ_{RH} and δ_T were dramatically weakened. Moreover, following irrigation, the correlations
 434 with T and RH for both MTs and SQTs were notably stronger than before the irrigation.
 435 This indicates that under drought, the temporal gradients in T and RH have a stronger
 436 impact on BVOC emissions than the absolute value of T and RH, in agreement with
 437 findings by Li et al. (2023). Here, we demonstrate that even a relatively minor precipitation
 438 event leads to T becoming the dominant factor in the BVOC emission rate, as expected
 439 under non-drought conditions. Interestingly, after irrigation, the highest r value for MTs
 440 was with T, but for SQTs, it was with RH.

441

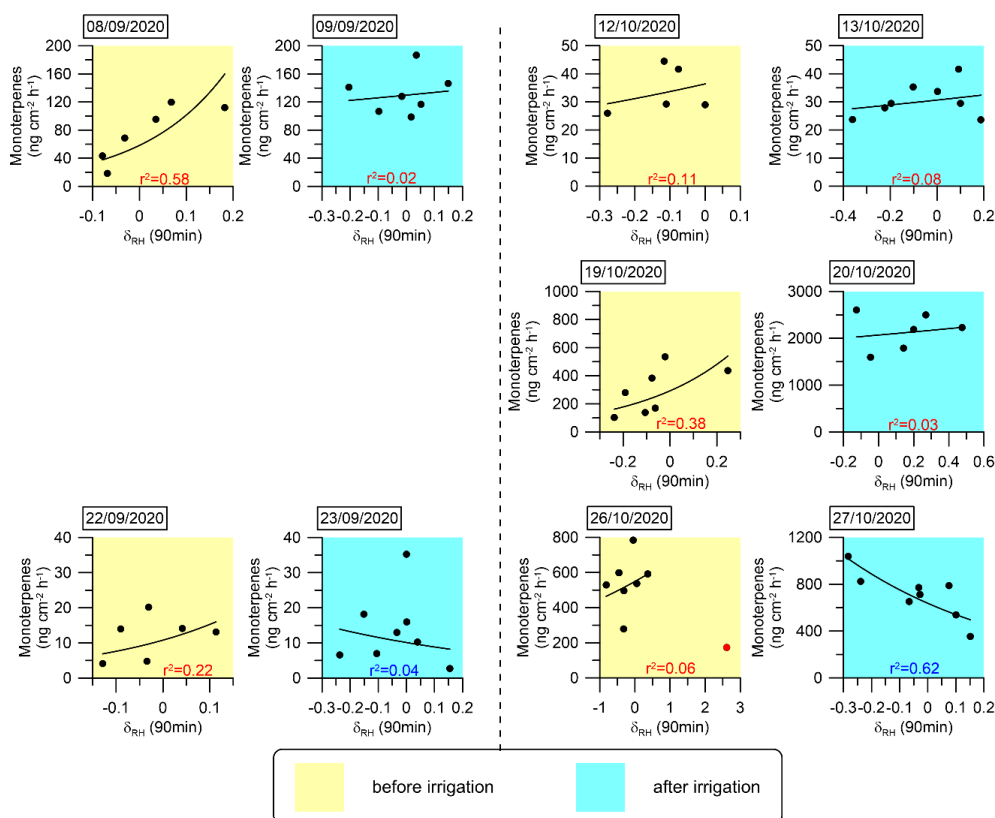
442 **Table 1.** Correlation between the emission rates of MTs and SQTs and the examined meteorological
 443 parameters. Presented are the Pearson’s r values for the correlation between MT/SQT emission rate and RH,
 444 T, δ_{RH} , and δ_T (green shading for SQT emissions and lavender shading for MT emissions). Blue and red
 445 shading indicates positive and negative correlation, respectively, and the darkness of the color indicates their
 446 values. The P-values for the correlation are shown in brackets.

Pearson's r value					
SQT	before irrigation	after irrigation	MT	before irrigation	after irrigation
vs RH	-0.22 (0.00)	-0.46 (0.00)	vs RH	-0.18 (0.11)	-0.44 (0.04)
vs T	0.33 (0.02)	0.42 (0.00)	vs T	0.20 (0.02)	0.46 (0.01)
vs δ_{RH}	0.53 (0.02)	-0.11 (0.00)	vs δ_{RH}	0.54 (0.01)	0.00 (0.00)
vs δ_T	-0.50 (0.02)	0.13 (0.00)	vs δ_T	-0.48 (0.01)	0.03 (0.00)



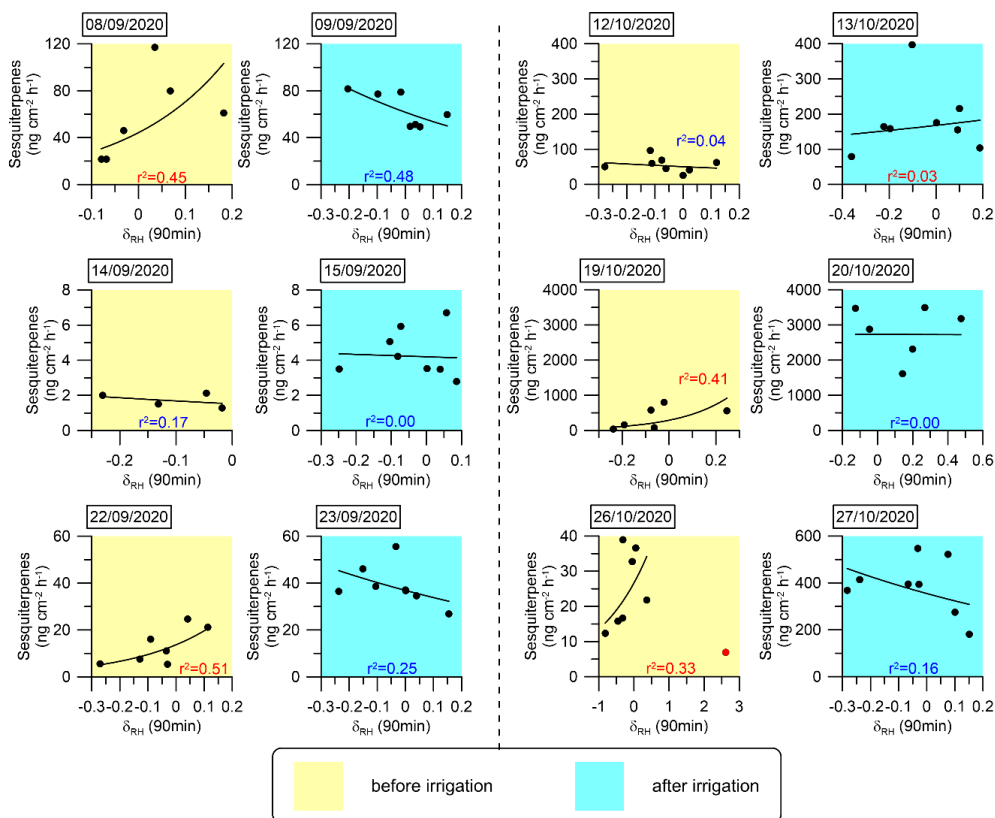
447 The analysis presented in Fig. 6 and Table 1 reinforces the finding that
448 instantaneous changes in meteorological parameters, particularly δ_{RH} , serve as a better
449 proxy for BVOC emission rate under drought conditions. This finding suggests that
450 modeling BVOC emission rates under drought conditions can rely on δ_{RH} . In light of this
451 insight, we investigated the mathematical connection between δ_{RH} and the emission rates
452 of the MT and SQT fluxes. Exponential fitting corresponded with a relatively strong
453 correlation between these emission rates and δ_{RH} . Other fitting types used to test this
454 relationship are presented in Sect. S2. Figures 7 and 8 depict the exponential fitting curves
455 for MTs and SQTs, respectively. These curves are presented separately for each branch
456 and individually for drought and post-irrigation conditions. The r^2 for MTs with δ_{RH} ranged
457 from 0.06 to 0.58 ($r = 0.24$ – 0.76 , average 0.48) under drought, whereas following irrigation,
458 the corresponding correlations ranged from 0.02 to 0.62 ($r = -0.78$ – 0.28 , average -0.08).
459 For SQTs, the corresponding r^2 values were somewhat higher, ranging from 0.04 to 0.51 (r
460 = -0.41 – 0.67 , average $+0.33$) and 0.00 to 0.48 ($r = -0.69$ – 0.17 , average -0.24), under
461 drought and following irrigation, respectively.

462 Overall, these results suggest that while δ_{RH} is likely a better proxy for MT and
463 SQT emission rates (see Table 1 and Sect. S3), the correlation of δ_{RH} with these BVOCs
464 appears to be too weak to accurately predict their emission rates using δ_{RH} values in
465 atmospheric modeling. Additional study is needed before δ_{RH} can effectively serve as a
466 parameter for modeling BVOC emission rates.



467 **Figure. 7** Daily correlations between MT emission fluxes and δ_{RH} . An exponential fitting function was used
 468 to fit the curves. The coefficient of determination (r^2) for each day is marked in red or blue when the
 469 correlation is positive or negative, respectively.

470 Following irrigation, the correlations between the emission flux rates and δ_{RH}
 471 became more moderate (4 cases out of 11) or even negative (5 cases out of 11). This further
 472 demonstrates the high sensitivity of δ_{RH} 's effect on BVOC emissions to changes in water
 473 availability. Further research is required to examine the physiological and biochemical
 474 processes underlying the sensitivity of BVOC emission rates to δ_{RH} .



475

476 **Figure 8** Daily correlations between SQT emission fluxes and δ_{RH} . An exponential fitting function was used
 477 to fit the curves. The coefficient of determination (r^2) for each day is marked in red or blue when the
 478 correlation is positive or negative, respectively. The sample at 12:10 h on 26 Oct 2020 (marked in red) was
 479 not considered in the fitting curve for that day, because an extremely sharp increase in RH (from 10 to 31%)
 480 occurred within 10 min, which we considered an outlier.

481

482 4 Summary and conclusions

483 We investigated BVOC emission rates from branches of *Phillyrea latifolia* under both
 484 drought and minor irrigation conditions in the Eastern Mediterranean region, with the aim
 485 of assessing the influence of low precipitation levels and meteorological parameters on MT
 486 and SQT emission rates during drought stress. We found that leaf water content increases



487 gradually under prolonged periods of drought, indicating the plant's enhanced capacity for
488 water uptake under more severe drought conditions. The highest emission rate among all
489 detected MTs was of *cis*- β -ocimene, and among the detected SQTs, β -caryophyllene, α -
490 humulene, germacrene D, and α -farnesene. Both the MT and SQT emission rates were
491 significantly influenced by the availability of soil water. In response to irrigation, the MT
492 and SQT emission rates increased by 150% and 545%, respectively, indicating that even a
493 small amount of water (equivalent to 5.5–7 mm precipitation) can significantly impact their
494 emission rates.

495 This study highlights the complex way in which meteorological conditions affect
496 BVOC emissions under drought conditions. In line with Li et al.'s (2023) findings, under
497 drought, the instantaneous change of relative humidity, δ_{RH} , was the best proxy for BVOC
498 emission rates, considering the strong correlation between MTs and SQTs and δ_{RH} ($r =$
499 0.54 and 0.53, respectively). However, after a small amount of irrigation (equivalent to
500 5.5–7 mm precipitation), no correlation was observed between δ_{RH} and MT emission rate,
501 whereas a negative correlation with δ_{RH} was observed for SQT emission rate. The increase
502 in soil water availability led to T (for MTs) or RH (for SQTs) becoming the dominant
503 meteorological parameter affecting BVOC emission rate, making them the best proxies for
504 BVOC emission rates among all tested meteorological parameters. This indicates that
505 changes in water availability can dramatically alter the manner in which BVOC emissions
506 respond to meteorological conditions.

507 Hence, according to the conditions used in this study, under more severe drought,
508 δ_{RH} can serve as the best proxy for BVOC emission rate, whereas under more moderate
509 drought, either T or RH is the best proxy for BVOCs, in agreement with previous findings



510 presented in the companion paper by (Li et al., 2023). Our findings indicate that even a
511 small amount of precipitation can lead to a transition from a drought to non-drought regime
512 in terms of BVOC emission rates and the manner in which they respond to meteorological
513 conditions.

514

515 **Author contribution.** ET designed the experiments, QL and GL carried out the field
516 measurements, QL performed the data acquisition. QL performed the analytical analysis
517 together with EB and EL. QL and ET led the data analyses with contributions from all co-
518 authors. QL and ET prepared the manuscript with contributions from EB.

519

520 **Competing interests.** The authors declare that they have no conflict of interest.

521

522 **Acknowledgements**

523 This study was supported by the Israel Science Foundation, Grant Nos. 1787/15 and
524 543/22. Eran Tas holds the Joseph H. and Belle R. Braun Senior Lectureship in Agriculture.

525

526

527 **References**

- 528 Asensio D., Peñuelas J., Llusà J., Ogaya R., Filella I., 2007. Interannual and interseasonal soil CO₂
529 efflux and VOC exchange rates in a Mediterranean holm oak forest in response to
530 experimental drought. *Soil Biology and Biochemistry* 39(10),2471–2484.
531 <https://doi.org/10.1016/j.soilbio.2007.04.019>.
- 532 Aydin Y.M., Yaman B., Koca H., Dasedemir O., Kara M., Altiok H., Dumanoglu Y., Bayram A.,
533 Tolunay D., Odabasi M., Elbir T., 2014. Biogenic volatile organic compound (BVOC) emissions
534 from forested areas in Turkey: Determination of specific emission rates for thirty-one tree
535 species. *The Science of the total environment* 490,239–253.
536 <https://doi.org/10.1016/j.scitotenv.2014.04.132>.
- 537 Baldwin I.T., Halitschke R., Paschold A., Dahl C.C. von, Preston C.A., 2006. Volatile signaling in
538 plant-plant interactions: "talking trees" in the genomics era. *Science (New York, N.Y.)*
539 311(5762),812–815. <https://doi.org/10.1126/science.1118446>.



- 540 Berg A.R., Heald C.L., Huff Hartz K.E., Hallar A.G., Meddens A.J.H., Hicke J.A., Lamarque J.-F.,
541 Tilmes S., 2013. The impact of bark beetle infestations on monoterpene emissions and
542 secondary organic aerosol formation in western North America. *Atmos. Chem. Phys.*
543 13(6),3149–3161. <https://doi.org/10.5194/acp-13-3149-2013>.
- 544 Blande J.D., TIIVA P., OKSANEN E., Holopainen J.K., 2007. Emission of herbivore-induced volatile
545 terpenoids from two hybrid aspen (*Populus tremula* × *tremuloides*) clones under ambient
546 and elevated ozone concentrations in the field. *Glob Change Biol* 13(12),2538–2550.
547 <https://doi.org/10.1111/j.1365-2486.2007.01453.x>.
- 548 Bonn B., Magh R.-K., Rombach J., Kreuzwieser J., 2019. Biogenic isoprenoid emissions under
549 drought stress: Different responses for isoprene and terpenes. *Biogeosciences* 16(23),4627–
550 4645. <https://doi.org/10.5194/bg-16-4627-2019>.
- 551 Bracho-Nunez A., Knothe N.M., Welter S., Staudt M., Costa W.R., Liberato M.A.R., Piedade
552 M.T.F., Kesselmeier J., 2013. Leaf level emissions of volatile organic compounds (VOC) from
553 some Amazonian and Mediterranean plants. *Biogeosciences* 10(9),5855–5873.
554 <https://doi.org/10.5194/bg-10-5855-2013>.
- 555 Brillì F., Barta C., Fortunati A., Lerdau M., Loreto F., Centritto M., 2007. Response of isoprene
556 emission and carbon metabolism to drought in white poplar (*Populus alba*) saplings. *New*
557 *Phytol* 175(2),244–254. <https://doi.org/10.1111/j.1469-8137.2007.02094.x>.
- 558 Brillì F., Ciccioli P., Frattoni M., Prestininzi M., Spanedda A.F., Loreto F., 2009. Constitutive and
559 herbivore-induced monoterpenes emitted by *Populus x euroamericana* leaves are key
560 volatiles that orient *Chrysomela populi* beetles. *Plant, cell & environment* 32(5),542–552.
561 <https://doi.org/10.1111/j.1365-3040.2009.01948.x>.
- 562 Cai M., An C., Guy C., 2021. A scientometric analysis and review of biogenic volatile organic
563 compound emissions: Research hotspots, new frontiers, and environmental implications.
564 *Renewable and Sustainable Energy Reviews* 149(13),111317.
565 <https://doi.org/10.1016/j.rser.2021.111317>.
- 566 Calfapietra C., Fares S., Manes F., Morani A., Sgrigna G., Loreto F., 2013. Role of Biogenic Volatile
567 Organic Compounds (BVOC) emitted by urban trees on ozone concentration in cities: A
568 review. *Environmental pollution (Barking, Essex 1987)* 183,71–80.
569 <https://doi.org/10.1016/j.envpol.2013.03.012>.
- 570 Caser M., Chitarra W., D'Angiolillo F., Perrone I., Demasi S., Lovisolo C., Pistelli L., Pistelli L.,
571 Scariot V., 2019. Drought stress adaptation modulates plant secondary metabolite
572 production in *Salvia dolomitica* Codd. *Industrial Crops and Products* 129,85–96.
573 <https://doi.org/10.1016/j.indcrop.2018.11.068>.
- 574 Curci G., Beekmann M., Vautard R., Smiatek G., Steinbrecher R., Theloke J., Friedrich R., 2009.
575 Modelling study of the impact of isoprene and terpene biogenic emissions on European
576 ozone levels. *Atmospheric Environment* 43(7),1444–1455.
577 <https://doi.org/10.1016/j.atmosenv.2008.02.070>.
- 578 Dayan C., Fredj E., Misztal P.K., Gabay M., Guenther A.B., Tas E., 2020. Emission of biogenic
579 volatile organic compounds from warm and oligotrophic seawater in the Eastern
580 Mediterranean. *Atmos. Chem. Phys.* 20(21),12741–12759. <https://doi.org/10.5194/acp-20-12741-2020>.
- 581
- 582 Duhl T.R., Helmig D., Guenther A., 2008. Sesquiterpene emissions from vegetation: A review.
583 *Biogeosciences* 5(3),761–777. <https://doi.org/10.5194/bg-5-761-2008>.
- 584 Filella I., Primante C., Llusà J., Martín González A.M., Seco R., Farré-Armengol G., Rodrigo A.,
585 Bosch J., Peñuelas J., 2013. Floral advertisement scent in a changing plant-pollinators
586 market. *Scientific reports* 3,3434. <https://doi.org/10.1038/srep03434>.



- 587 Fitzky A.C., Kaser L., Peron A., Karl T., Graus M., Tholen D., Halbwirth H., Trimmel H.,
588 Pesendorfer M., Rewald B., Sandén H., 2023. Same, same, but different: Drought and salinity
589 affect BVOC emission rate and alter blend composition of urban trees. *Urban Forestry &
590 Urban Greening* 80(7),127842. <https://doi.org/10.1016/j.ufug.2023.127842>.
- 591 Fortunati A., Barta C., Brillì F., Centritto M., Zimmer I., Schnitzler J.-P., Loreto F., 2008. Isoprene
592 emission is not temperature-dependent during and after severe drought-stress: A
593 physiological and biochemical analysis. *The Plant journal for cell and molecular biology*
594 55(4),687–697. <https://doi.org/10.1111/j.1365-313X.2008.03538.x>.
- 595 Genard-Zielinski A.-C., Boissard C., Fernandez C., Kalogridis C., Lathière J., Gros V., Bonnaire N.,
596 Ormeño E., 2015. Variability of BVOC emissions from a Mediterranean mixed forest in
597 southern France with a focus on *Quercus pubescens*. *Atmos. Chem. Phys.*
598 15(1),431–446. <https://doi.org/10.5194/acp-15-431-2015>.
- 599 Genard-Zielinski A.-C., Boissard C., Ormeño E., Lathière J., Reiter I.M., Wortham H., Orts J.-P.,
600 Temime-Roussel B., Guenet B., Bartsch S., Gauquelin T., Fernandez C., 2018. Seasonal
601 variations of *Quercus pubescens*; isoprene emissions from an *in natura* forest under drought stress and sensitivity to future climate change in the
602 Mediterranean area. *Biogeosciences* 15(15),4711–4730. <https://doi.org/10.5194/bg-15-4711-2018>.
- 603 Geron C., Daly R., Harley P., Rasmussen R., Seco R., Guenther A., Karl T., Gu L., 2016. Large
604 drought-induced variations in oak leaf volatile organic compound emissions during PINOT
605 NOIR 2012. *Chemosphere* 146,8–21. <https://doi.org/10.1016/j.chemosphere.2015.11.086>.
- 606 Giorgi F., Lionello P., 2008. Climate change projections for the Mediterranean region. *Global and
607 Planetary Change* 63(2-3),90–104. <https://doi.org/10.1016/j.gloplacha.2007.09.005>.
- 608 Goldstein A.H., McKay M., Kurpius M.R., Schade G.W., Lee A., Holzinger R., Rasmussen R.A.,
609 2004. Forest thinning experiment confirms ozone deposition to forest canopy is dominated
610 by reaction with biogenic VOCs. *Geophys. Res. Lett.* 31(22),22,123.
611 <https://doi.org/10.1029/2004GL021259>.
- 612 Greenberg J.P., Asensio D., Turnipseed A., Guenther A.B., Karl T., Gochis D., 2012. Contribution
613 of leaf and needle litter to whole ecosystem BVOC fluxes. *Atmospheric Environment* 59,302–
614 311. <https://doi.org/10.1016/j.atmosenv.2012.04.038>.
- 615 Guenther A., 2013. Biological and Chemical Diversity of Biogenic Volatile Organic Emissions into
616 the Atmosphere. *ISRN Atmospheric Sciences* 2013(19),1–27.
617 <https://doi.org/10.1155/2013/786290>.
- 618 Guenther A., Hewitt C.N., Erickson D., Fall R., Geron C., Graedel T., Harley P., Klinger L., Lerdau
619 M., McKay W.A., Pierce T., Scholes B., Steinbrecher R., Tallamraju R., Taylor J., Zimmerman
620 P., 1995. A global model of natural volatile organic compound emissions. *J. Geophys. Res.*
621 100(D5),8873–8892.
- 622 Guenther A.B., Jiang X., Heald C.L., Sakulyanontvittaya T., Duhl T., Emmons L.K., Wang X., 2012.
623 The Model of Emissions of Gases and Aerosols from Nature version 2.1 (MEGAN2.1): An
624 extended and updated framework for modeling biogenic emissions. *Geosci. Model Dev.*
625 5(6),1471–1492. <https://doi.org/10.5194/gmd-5-1471-2012>.
- 626 Han Z., Zhang Y., Zhang H., Ge X., Gu D., Liu X., Bai J., Ma Z., Tan Y., Zhu F., Xia S., Du J., Tan Y.,
627 Shu X., Tang J., Sun Y., 2022. Impacts of Drought and Rehydration Cycles on Isoprene
628 Emissions in *Populus nigra* Seedlings. *International journal of environmental research and
629 public health* 19(21). <https://doi.org/10.3390/ijerph192114528>.
- 630 Holopainen J.K., Gershenson J., 2010. Multiple stress factors and the emission of plant VOCs.
631 *Trends in plant science* 15(3),176–184. <https://doi.org/10.1016/j.tplants.2010.01.006>.
- 632
633



- 634 Jiang X., Guenther A., Potosnak M., Geron C., Seco R., Karl T., Kim S., Gu L., Pallardy S., 2018.
635 Isoprene Emission Response to Drought and the Impact on Global Atmospheric Chemistry.
636 Atmospheric environment (Oxford, England 1994) 183,69–83.
637 <https://doi.org/10.1016/j.atmosenv.2018.01.026>.
- 638 Kesselmeier J., Staudt M., 1999. Biogenic Volatile Organic Compounds (VOC): An Overview on
639 Emission, Physiology and Ecology. *Journal of Atmospheric Chemistry* 33,23–88.
- 640 Li Q., Gabay M., Dayan C., Misztal P., Guenther A., Fredj E., Tas E., 2023. Intraday instantaneous
641 changes in relative humidity as a key proxy for the mixing ratio of biogenic volatile organic
642 compounds over vegetation under drought conditions. *Atmos. Chem. Phys.*
- 643 Li Q., Gabay M., Rubin Y., Fredj E., Tas E., 2018. Measurement-based investigation of ozone
644 deposition to vegetation under the effects of coastal and photochemical air pollution in the
645 Eastern Mediterranean. *Science of The Total Environment* 645,1579–1597.
646 <https://doi.org/10.1016/j.scitotenv.2018.07.037>.
- 647 Lionello P., 2012. *The Climate of the Mediterranean Region: From the Past to the Future:*
648 Elsevier.
- 649 Llusia J., Roahtyn S., Yakir D., Rotenberg E., Seco R., Guenther A., Peñuelas J., 2016.
650 Photosynthesis, stomatal conductance and terpene emission response to water availability
651 in dry and mesic Mediterranean forests. *Trees* 30(3),749–759.
652 <https://doi.org/10.1007/s00468-015-1317-x>.
- 653 Llusia J., Peñuelas J., 2000. Seasonal patterns of terpene content and emission from seven
654 Mediterranean woody species in field conditions. *American J of Botany* 87(1),133–140.
655 <https://doi.org/10.2307/2656691>.
- 656 Medrano H., Escalona J.M., Bota J., Gulías J., Flexas J., 2002. Regulation of photosynthesis of C3
657 plants in response to progressive drought: Stomatal conductance as a reference parameter.
658 *Annals of botany* 89 Spec No(7),895–905. <https://doi.org/10.1093/aob/mcf079>.
- 659 MIYASHITA K., TANAKAMARU S., MAITANI T., KIMURA K., 2005. Recovery responses of
660 photosynthesis, transpiration, and stomatal conductance in kidney bean following drought
661 stress. *Environmental and Experimental Botany* 53(2),205–214.
662 <https://doi.org/10.1016/j.envexpbot.2004.03.015>.
- 663 Monson R.K., Jaeger C.H., Adams W.W., Driggers E.M., Silver G.M., Fall R., 1992. Relationships
664 among Isoprene Emission Rate, Photosynthesis, and Isoprene Synthase Activity as Influenced
665 by Temperature. *PLANT PHYSIOLOGY* 98(3),1175–1180.
- 666 Niinemets U., Loreto F., Reichstein M., 2004. Physiological and physicochemical controls on
667 foliar volatile organic compound emissions. *Trends in plant science* 9(4),180–186.
668 <https://doi.org/10.1016/j.tplants.2004.02.006>.
- 669 Niinemets U., Monson R.K., 2013. *Biology, controls and models of tree volatile organic*
670 *compound emissions.* Dordrecht: Springer.
- 671 Nobel P.S., 1999. *Physicochemical & environmental plant physiology.* 2nd ed. San Diego:
672 Academic Press.
- 673 Núñez L., Plaza J., Pérez-Pastor R., Pujadas M., Gimeno B.S., Bermejo V., García-Alonso S., 2002.
674 High water vapour pressure deficit influence on *Quercus ilex* and *Pinus pinea* field
675 monoterpene emission in the central Iberian Peninsula (Spain). *Atmospheric Environment*
676 36(28),4441–4452. [https://doi.org/10.1016/S1352-2310\(02\)00415-6](https://doi.org/10.1016/S1352-2310(02)00415-6).
- 677 Owen S., Boissard C., Street R.A., Duckham S.C., Csiky O., Hewitt C.N., 1997. Screening of 18
678 Mediterranean plant species for volatile organic compound emissions. *Atmospheric*
679 *Environment* 31,101–117. [https://doi.org/10.1016/S1352-2310\(97\)00078-2](https://doi.org/10.1016/S1352-2310(97)00078-2).



- 680 Owen S.M., Hewitt C.N., 2000. Extrapolating branch enclosure measurements to estimates of
681 regional scale biogenic VOC fluxes in the northwestern Mediterranean basin. *J. Geophys.*
682 *Res.* 105(D9),11573–11583. <https://doi.org/10.1029/1999JD901154>.
- 683 PEGORARO E., REY A.N.A., ABRELL L., van HAREN J., LIN G., 2006. Drought effect on isoprene
684 production and consumption in Biosphere 2 tropical rainforest. *Glob Change Biol* 12(3),456–
685 469. <https://doi.org/10.1111/j.1365-2486.2006.01112.x>.
- 686 Peñuelas J., Munné-Bosch S., 2005. Isoprenoids: An evolutionary pool for photoprotection.
687 *Trends in plant science* 10(4),166–169. <https://doi.org/10.1016/j.tplants.2005.02.005>.
- 688 Peñuelas J., Rutishauser T., Filella I., 2009. Ecology. Phenology feedbacks on climate change.
689 *Science (New York, N.Y.)* 324(5929),887–888. <https://doi.org/10.1126/science.1173004>.
- 690 Peñuelas J., Staudt M., 2010. BVOCs and global change. *Trends in plant science* 15(3),133–144.
691 <https://doi.org/10.1016/j.tplants.2009.12.005>.
- 692 Potosnak M.J., LeStourgeon L., Pallardy S.G., Hosman K.P., Gu L., Karl T., Geron C., Guenther
693 A.B., 2014. Observed and modeled ecosystem isoprene fluxes from an oak-dominated
694 temperate forest and the influence of drought stress. *Atmospheric Environment* 84,314–
695 322. <https://doi.org/10.1016/j.atmosenv.2013.11.055>.
- 696 Ryan A.C., Hewitt C.N., Possell M., Vickers C.E., Purnell A., Mullineaux P.M., Davies W.J., Dodd
697 I.C., 2014. Isoprene emission protects photosynthesis but reduces plant productivity during
698 drought in transgenic tobacco (*Nicotiana tabacum*) plants. *New Phytol* 201(1),205–216.
699 <https://doi.org/10.1111/nph.12477>.
- 700 Saunders S.M., Jenkin M.E., Derwent R.G., Pilling M.J., 2003. Protocol for the development of
701 the Master Chemical Mechanism, MCM v3 (Part A): tropospheric degradation of non-
702 aromatic volatile organic compounds. *Atmos. Chem. Phys.* 3,161–180.
- 703 Saunier A., Ormeño E., Boissard C., Wortham H., Temime-Roussel B., Lecareux C., Armengaud A.,
704 Fernandez C., 2017. Effect of mid-term drought on *Quercus pubescens* BVOCs'
705 BVOCs' emission seasonality and their dependency on light and/or temperature. *Atmos.*
706 *Chem. Phys.* 17(12),7555–7566. <https://doi.org/10.5194/acp-17-7555-2017>.
- 707 Schade G.W., Goldstein A.H., Lamanna M.S., 1999. Are monoterpene emissions influenced by
708 humidity? *Geophys. Res. Lett.* 26(14),2187–2190.
- 709 Seco R., Karl T., Turnipseed A., Greenberg J., Guenther A., Llusia J., Peñuelas J., Dicken U.,
710 Rotenberg E., Kim S., Yakir D., 2017. Springtime ecosystem-scale monoterpene fluxes from
711 Mediterranean pine forests across a precipitation gradient. *Agricultural and Forest*
712 *Meteorology* 237-238,150–159. <https://doi.org/10.1016/j.agrformet.2017.02.007>.
- 713 Sindelarova K., Granier C., Bouarar I., Guenther A., Tilmes S., Stavrakou T., Müller J.-F., Kuhn U.,
714 Stefani P., Knorr W., 2014. Global data set of biogenic VOC emissions calculated by the
715 MEGAN model over the last 30 years. *Atmos. Chem. Phys.* 14(17),9317–9341.
716 <https://doi.org/10.5194/acp-14-9317-2014>.
- 717 Staudt M., Mandl N., Joffre R., Rambal S., 2001. Intraspecific variability of monoterpene
718 composition emitted by *Quercus ilex* leaves. *Can. J. For. Res.* 31(1),174–180.
719 <https://doi.org/10.1139/x00-153>.
- 720 Street R.A., Owen S., Duckham S.C., Boissard C., Hewitt C.N., 1997. Effect of habitat and age on
721 variations in volatile organic compound (VOC) emissions from *Quercus ilex* and *Pinus pinea*.
722 *Atmospheric Environment* 31,89–100. [https://doi.org/10.1016/S1352-2310\(97\)00077-0](https://doi.org/10.1016/S1352-2310(97)00077-0).
- 723 Tingey D., Turner D., Weber J., 1990. Factors Controlling the Emissions of Monoterpenes and
724 Other Volatile Organic Compounds: U.S. Environmental Protection Agency, Washington, D.C.
725 EPA/600/D-90/195 (NTIS PB91136622).
- 726 Vilagrosa A., Bellot J., Vallejo V.R., Gil-Pelegrin E., 2003. Cavitation, stomatal conductance, and
727 leaf dieback in seedlings of two co-occurring Mediterranean shrubs during an intense

<https://doi.org/10.5194/egusphere-2024-529>

Preprint. Discussion started: 20 March 2024

© Author(s) 2024. CC BY 4.0 License.



728 drought. Journal of experimental botany 54(390),2015–2024.
729 <https://doi.org/10.1093/jxb/erg221>.
730